Velocity and Velocity-Difference Distributions in Burgers Turbulence

Stanislav Boldyrev,[1] Timur Linde,[1] and Alexandre Polyakov[2]

[1]*Department of Astronomy and Astrophysics, University of Chicago, Chicago, Illinois 60637, USA*
[2]*Joseph Henry Laboratories, Princeton University, Princeton, New Jersey 08544, USA*
(Received 28 May 2003; published 28 October 2004)

We consider the one-dimensional Burgers equation randomly stirred at large scales by a Gaussian short-time correlated force. Using the method of dissipative anomalies, we obtain velocity and velocity-difference probability density functions and confirm the results with high-resolution numerical simulations.

Introduction.—The one-dimensional Burgers equation with a random external force,

$$u_t + u u_x = \nu u_{xx} + f(x, t), \qquad (1)$$

is a simple model of turbulence, where $u(x, t)$ is a one-dimensional velocity field, and ν is small viscosity. The external force is assumed to be Gaussian, with zero mean and white-in-time covariance,

$$\langle f(x, t) f(x', t') \rangle = \kappa(x - x') \delta(t - t'), \qquad (2)$$

where $\kappa(y)$ should be specified. We assume that it is an analytic function at $y \to 0$ with the characteristic scale L; nonanalytic forms of κ have been considered as well [1]. This model has attracted considerable attention since it is believed to be exactly solvable [1–14].

Let us introduce the characteristic function of the N-point velocity distribution, $Z_N(\lambda_1, x_1; \ldots; \lambda_N, x_N; t) = \langle \exp[\lambda_1 u(x_1, t) + \cdots + \lambda_N u(x_N, t)] \rangle$. As was shown in [2], it obeys the master equation that one derives by differentiating this function with respect to t, and by using Eq. (1),

$$\frac{\partial Z_2}{\partial t} = -\lambda_i \frac{\partial}{\partial \lambda_i} \frac{1}{\lambda_i} \frac{\partial Z_2}{\partial x_i} + \frac{1}{2} \lambda_i \lambda_j \kappa(x_i - x_j) Z_2 + D, \qquad (3)$$

where the summation over repeated indices is assumed.

The last term in Eq. (3) denotes the contribution of the dissipative terms. Although the method of our Letter is valid for the general case of the N-point characteristic function, we concentrate on the case $N = 2$, where the solution is easy to find. In this case, $D = \nu \langle (\lambda_1 u_{x_1 x_1} + \lambda_2 u_{x_2 x_2}) \exp[\lambda_1 u(x_1, t) + \lambda_2 u(x_2, t)] \rangle$. This term does not vanish in the limit of infinitely large Reynolds number, $\nu \to 0$; rather, it has a finite value, because the velocity field develops singularities, shocks, where large velocity gradients are balanced by the small viscosity. It has been proposed in [2] that the origin of this term is analogous to the origin of anomalies in quantum field theories, and it has been suggested that this term can be expressed linearly through the Z function. Namely, the following ansatz should be true inside any $N \geq 2$ point correlation function

$$A \equiv \lim_{\nu \to 0} \nu \lambda u_{xx} e^{\lambda u(x)} = \left[\frac{a}{2} + \frac{b - 1}{\lambda} \frac{\partial}{\partial x} \right] e^{\lambda u(x)}. \qquad (4)$$

The right-hand side of (4) contains the simplest linear in $e^{\lambda u}$ terms that are consistent with translation, scale, and Galilean invariance [2,3]. The higher-derivative terms are not allowed since they would change the structure of Eq. (3) and may lead to additional, nonphysical solutions. The parameters a and b, which we call "anomalies," should be found from the requirement that the stationary solution of Eq. (3) correspond to a positive, finite, and normalizable probability density function (PDF), similar to the eigenvalue problem in quantum mechanics. The other condition is nonpositivity of the dissipation, $D \leq 0$. These two conditions restrict the values of the anomalies considerably. It has been shown in [3] that the admissible solution exists for a one-parameter family $\{b, a(b)\}$, where $3/4 \leq b \leq 1$ and the corresponding interval for the a anomaly is $0 \geq a \geq -0.45$.

The corresponding scale-invariant solution for the velocity-difference PDF, $w(\Delta u / y)$, where $\Delta u = u(x_1) - u(x_2) \ll u_{\text{rms}}$ and $y = x_1 - x_2 \ll L$ can be found from (3). It has a peculiar structure that was first qualitatively established in numerical simulations [1] and was confirmed by a variety of analytical methods [2–7]. It decays hyperexponentially fast for the large positive argument, $w(z) \propto \exp(-z^3/3)$, and has an algebraic tail for the large negative argument, $w(z) \propto |z|^{-2b-1}$ (see Sec. II). This behavior is understood since due to the nonlinear term in Eq. (1), positive gradients decrease in the course of time, while negative gradients become stronger. Therefore, large negative velocity gradients are more probable than large positive ones.

According to the allowed values of the anomaly b in model (4), the distribution density should decay slower than $|z|^{-3}$ for $z \to -\infty$. However, the geometric consideration of preshock events producing large negative velocity gradients, proposed in [7,8], suggested the asymptotic $|z|^{-7/2}$. Lagrangian simulations of only the left tail of the PDF agreed with the latter result [12–14].

So far, no analytical derivation of the full velocity-difference PDF decaying as $|z|^{-7/2}$ was available. The direct numerical simulations of Eq. (1), carried out in [9,10], have not convincingly reproduced such a PDF either. The form of the PDF has therefore remained a subject of controversy.

In this Letter we propose that the PDF is not unique. In an infinite system, where the Galilean invariance holds, the anomaly has the form (4). In the finite-size systems, investigated in [12–14], the global Galilean invariance is broken and the weak Galilean principle should be applied. In this case the form of the anomaly is different from (4), and the solution with the asymptotics $|z|^{-7/2}$ may be allowed. We derive the corresponding velocity and velocity-difference PDFs. Next, we conduct extensive numerical simulations of Eq. (1), using a high-resolution shock capturing scheme. The results agree well with our analytical prediction. Section II presents the theory, while Sec. III the numerical simulations.

Velocity and velocity-difference PDFs.—The resolution of the controversy mentioned above is based on the fact that the form (4) of the anomaly is dictated by the strong form of the Galilean principle (see below) while the arguments of [7,8] as well as numerical results [12–14] are correct only when the weak G principle applies. The strong Galilean principle is the requirement that in the infinite system, taking velocity to zero at infinity does not break the Galilean symmetry in the middle. This requirement is analogous to the absence of the spontaneous symmetry breaking in magnetic systems. For the systems considered in [7,8,12–14] this strong G principle obviously does not hold. The reason is that the size of the systems is of the same order as the correlation length of the force. Therefore, the velocities in the middle of the system are correlated to those at the boundary. The same argument works for the periodic case, in which the Galilean symmetry is broken by the condition $u_0 = \int u dx = 0$.

So, the results in [2,7,8,12–14] refer to the different dynamical systems and that explains the discrepancy. The natural question is whether we can apply the methods of [2] for the case in which the strong G symmetry is broken. This is important because the method of dissipative anomalies is the only known nonperturbative way to solve Burgers turbulence. In this case we still have the weak G symmetry, which says that all correlation functions are G symmetric, provided that we average them over u_0. This is of course always true, but how do we impose this condition?

Let us notice that the correlation functions calculated at the fixed u_0 have the property

$$\langle e^{\sum \lambda_j u(x_j,t)} \rangle_{u_0} = e^{u_0 \sum \lambda_j} \langle e^{\sum \lambda_j u(x_j,t)} \rangle_0. \qquad (5)$$

Hence, if we integrate over u_0 the correlations must have the form

$$\langle e^{\sum \lambda_j u(x_j,t)} \rangle = 2\pi \delta\left(\sum \lambda_j\right) \langle e^{\sum \lambda_j u(x_j,t)} \rangle_0. \qquad (6)$$

The master Eq. (3) must allow this ansatz; namely, the proportionality to the $\delta(\sum \lambda_j)$ must be consistent with the equation. This is obviously so with the anomaly (4), but this also allows a more general form of the anomaly. Let us look at the expression

$$\tilde{A} = A + c\lambda \frac{\partial}{\partial \lambda} e^{\lambda u}; \qquad (7)$$

it adds the term $\tilde{D} = c \sum \lambda_j \partial Z / \partial \lambda_j$ to the right-hand side of Eq. (3). When $Z = \delta(\sum \lambda_j) Z_0$, we have $\tilde{D} = c(\sum \lambda_j \partial Z_0 / \partial \lambda_j - Z_0)\delta(\sum \lambda_j)$, where we used the identity $x\delta'(x) = -\delta(x)$. It is important to notice that any other function of λ or higher power of $\partial/\partial\lambda$ would break the ansatz. Anomalies of the form (7) have been considered in relation to incompressible turbulence by Yakhot [15].

The restrictions on the coefficients a, b, and c can be obtained from the equation for the velocity-difference PDF. To write this equation, substitute the dissipative term (7) into Eq. (3). In the Galilean-invariant limit, the statistics of velocity differences are separated from those of the mean velocity field. Let us change the variables, $\lambda_1 = \Lambda + \mu$, $\lambda_2 = \Lambda - \mu$, $x_1 = X + y/2$, and $x_2 = X - y/2$ and assume that $\Lambda \ll \mu$ and $y \ll L$. The latter condition allows us to expand $\kappa(y) \simeq \kappa_0 - \kappa_2 y^2/2$. In this limit, the master Eq. (3) becomes

$$\frac{\partial^2 Z_2}{\partial \mu \partial y} - \frac{2b}{\mu} \frac{\partial Z_2}{\partial y} -$$

$$2\Lambda^2 \kappa_0 Z_2 - \frac{\kappa_2 \mu^2 y^2}{2} Z_2 = c\mu \frac{\partial Z_2}{\partial \mu} + c\Lambda \frac{\partial Z_2}{\partial \Lambda} + aZ_2, \qquad (8)$$

where we consider the stationary case, $\partial_t Z_2 = 0$. In the finite-size system with $u_0 = 0$, we assume the weak G symmetry and look for the solution in the form $Z_2 = Z_+(\Lambda)Z_-(\mu, y)$. [The strong G symmetry would imply $Z_+(\Lambda) \sim \delta(\Lambda)$ and the solution might be different.] Substituting this into Eq. (8) we get the following set of equations for the characteristic functions Z_+ and Z_-:

$$-2\Lambda^2 \kappa_0 Z_+ = c\Lambda \frac{\partial Z_+}{\partial \Lambda}, \qquad (9)$$

$$\frac{\partial^2 Z_-}{\partial \mu \partial y} - \frac{2b}{\mu} \frac{\partial Z_-}{\partial y} - \frac{\kappa_2 \mu^2 y^2}{2} Z_- = c\mu \frac{\partial Z_-}{\partial \mu} + aZ_-. \qquad (10)$$

The solution of Eq. (9) corresponds to a positive and normalizable PDF only when $c < 0$, and the solution is a Gaussian. Its Laplace transform then gives the velocity probability density function

$$P(U) = \sqrt{\frac{-c}{\pi \kappa_0}} \exp\left(\frac{cU^2}{\kappa_0}\right), \qquad (11)$$

where $U = [u(x_1) + u(x_2)]/2$. Since the point separation is much smaller than the force correlation length, $P(U)$

becomes the one-point probability density function of the velocity field. Strictly speaking, expression (11) is phenomenological; it is expected to match the velocity PDF only in the region $U \ll U_{\mathrm{rms}}$. For larger U the velocity PDF may be not universal. We compare this result with the simulations in Sec. III.

Equation (10) is more complicated, but it can be simplified if we are looking for the solution in the scale-invariant form, $Z_-(\mu, y) = \Phi(x)$, where $x = \mu y$,

$$x\Phi'' + (1 - 2b)\Phi' - \frac{\kappa_2}{2}x^2\Phi = a\Phi + cx\frac{\partial}{\partial x}\Phi. \quad (12)$$

To rewrite this equation in the velocity space, let us Laplace transform the Φ function,

$$\Phi(x) = \int_{-\infty}^{+\infty} w(\tilde{z})\exp(x\tilde{z})d\tilde{z}. \quad (13)$$

The function $w(\tilde{z})$ is then related to the velocity-difference probability density function, $W(\Delta u, y)$, as $W(\Delta u, y) = w(\Delta u/y)/y$. The equation for w is readily obtained by substituting (13) into (12). Introducing the dimensionless variable $z = \tilde{z}(\kappa_2/2)^{-1/3}$, we thus get

$$w'' + z^2 w' + (1 + 2b)zw = -\tilde{a}w + \tilde{c}(zw)', \quad (14)$$

where the derivatives are with respect to z, and $\tilde{a} = a(\kappa_2/2)^{-1/3}$ and $\tilde{c} = c(\kappa_2/2)^{-1/3}$. Asymptotics of the solution at $|z| \to \infty$ can be found from Eq. (14),

$$w \sim z^{(2b-1)}\exp(-z^3/3 + \tilde{c}z^2/2), \qquad z \to +\infty, \quad (15)$$

$$w \sim |z|^{-(2b+1)}, \qquad z \to -\infty; \quad (16)$$

they have the form that we already discussed in the introduction.

Ideally, we should be able to derive all the anomalies a, b, and c from our theory. At present we are not able to do this, so in the next section we turn to numerical simulations.

In general, the anomalies a, b, and c should satisfy the requirement that Eq. (14) have a positive and a normalizable solution and that the dissipation is nonpositive, $\tilde{a}w + 2(b-1)zw - \tilde{c}(zw)' \leq 0$ [3]. This eigenvalue problem thus has a two-parameter family of solutions.

Note that the geometric approach of [7,8,11–14] proposed the asymptotic for negative velocity differences, $w \sim |z|^{-7/2}$. This condition is satisfied by $b = 5/4$. This value was not allowed by the condition of nonpositivity of the dissipation in the theory based on (4), but with the new expression for the anomaly (7) this value is admissible. For $b = 5/4$, Eq. (14) can be solved numerically, leading to the approximate window of acceptable values, $-0.37 \leq \tilde{c} \leq -0.025$, which turns out to be consistent with (11). We now find the values of the anomalies from numerical simulations of Eq. (1).

Numerical results.—We perform numerical simulations of Eq. (1) in a periodic interval of length $L = 1$ containing 10^6 grid points. The used numerical scheme is the
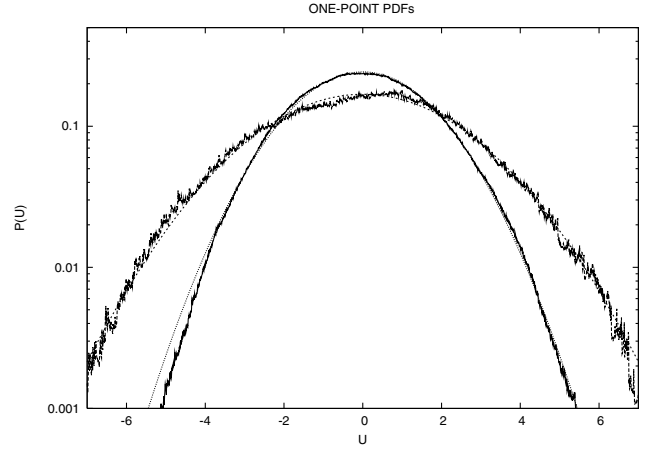

FIG. 1. Numerical and analytical one-point PDFs for two runs, $n = 5$ and $n = 10$. The broader curves correspond to the run $n = 10$. The plot is in log-lin scale.

standard shock capturing, total variation diminishing (TVD) scheme with nonlinear, limited solution reconstruction [16]. For nonlinear, scalar equations the scheme is provably TV stable, monotonicity preserving, and second-order accurate in the L_p, $p < \infty$, norm. To resolve discontinuous solutions the scheme uses nonlinear numerical viscosity that appears only inside the shocks. This dissipation mechanism ensures that the shocks are restricted to two to three grid points. The external force is generated as

$$f(x) = \sum_{k=1}^{m} A(k)[\xi_k \sin(2\pi kx) + \eta_k \cos(2\pi kx)], \quad (17)$$

where ξ_k and η_k are independent Gaussian random variables with mean 0 and covariance 1. The amplitude of the force is $A(k) = k[\exp(-k^2/n^2)/\tau]^{1/2}$, where τ is the force renewal time; in our simulations we had $\tau = 10^{-5}$, while
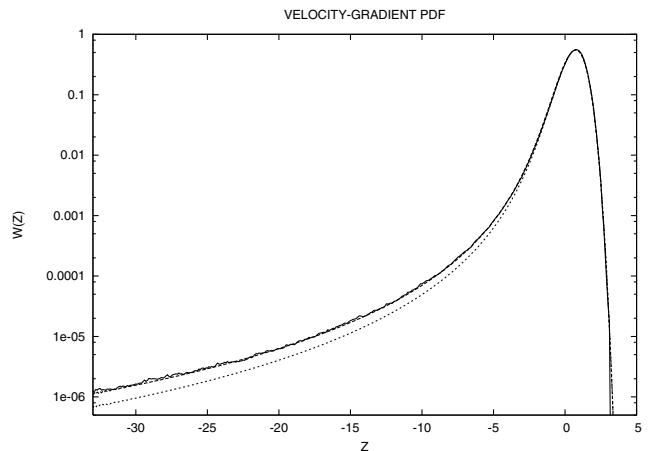

FIG. 2. Velocity-gradient PDF for the run $n = 5$. The analytical curves correspond to the solution of Eq. (14) with $b = 1.19$ (dashed line) and $b = 5/4$ (dotted line). In both cases, $\tilde{c} = -0.3$. The plot is in log-lin scale.

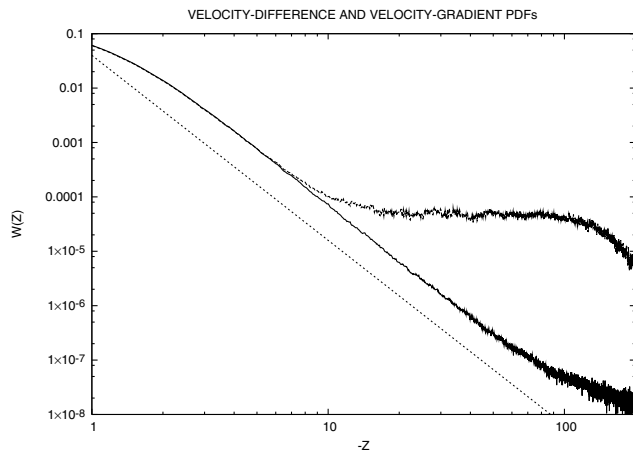VELOCITY-DIFFERENCE AND VELOCITY-GRADIENT PDFs

FIG. 3. The left tails of the velocity-gradient PDF (lower curve) and of the velocity-difference PDF (upper curve, point separation $\Delta x = 10^{-3}$). For the reader's orientation, the straight line has the slope -3.4.

the integration time step was $t_0 = 10^{-7}$. We used $m = 10$ and performed a series of runs for $n = 5, 10$. In this Letter we mainly present the results averaged over five independent runs with $n = 5$, and with the integration time $t = 2$ each.

We found that the one-point PDF can be best matched by the solution of Eq. (11), with the choice $\tilde{c} = -0.3$. Formula (11) gives

$$P(U) = \sqrt{\frac{0.3\kappa_2^{1/3}}{2^{1/3}\pi\kappa_0}}\exp\left(-\frac{0.3\kappa_2^{1/3}}{2^{1/3}\kappa_0}U^2\right), \qquad (18)$$

and Fig. 1 shows its good agreement with the simulations for both $n = 5$ and $n = 10$. As expected, the best agreement is seen in the top parts of the curves; the tails of the PDF seem to be nonuniversal.

Once the c anomaly is given, we find the anomaly b by matching the numerically obtained velocity-difference PDF with the solution of Eq. (14); see Figs. 2 and 3. The best match to the *whole* PDF is given by $b \approx 1.19$ which is slightly less than the value $b = 5/4$, predicted in [7,8,11–14], and leads to the left-tail exponent -3.38. The solution of Eq. (14) with the value $b = 5/4$ is less consistent with our simulations. Although the reason for this discrepancy is quite intriguing and is not clear to us, our numerical resolution is not high enough to distinguish between the two asymptotics, -3.5 and -3.38. Therefore, more extensive numerical work is required to understand this difference.

Once the anomalies c and b are found, the a anomaly is obtained from the eigenvalue problem (14), which gives $\tilde{a} \approx -0.65$.

Conclusions.—We have found that our analytical model (14) with parameters $\tilde{a} \approx -0.65$, $b \approx 1.19$, and $\tilde{c} \approx -0.3$ provides an excellent fit to the numerically obtained velocity and velocity-difference PDFs of Burgers turbulence. For an important numerical check, one can directly find the form of the anomalies by numerically constructing conditional probabilities of shock amplitudes for given velocity gradients on the left and on the right of the shock [8]. We plan to address this question in the future with more extensive simulations.

We also believe that the method of dissipative anomalies can be generalized for turbulence with pressure and can be applicable in more than one dimension. We currently conduct the corresponding simulations; the results will be reported elsewhere. Practically, the Burgers model is expected to work for strongly compressible flows, i.e., in astrophysical application, such as supersonic turbulence in cold molecular clouds [17,18].

[1] A. Chekhlov and V. Yakhot, Phys. Rev. E **52**, 5681 (1995); V. Yakhot and A. Chekhlov, Phys. Rev. Lett. **77**, 3118 (1996).
[2] A. Polyakov, Phys. Rev. E **52**, 6183 (1995).
[3] S. Boldyrev, Phys. Rev. E **55**, 6907 (1997); Phys. Plasmas **5**, 1681 (1998).
[4] V. Gurarie and A. Migdal, Phys. Rev. E **54**, 4908 (1996); V. Gurarie, hep-th/9606089.
[5] J.-P. Bouchaud and M. Mézard, Phys. Rev. E **54**, 5116 (1996).
[6] E. Balkovsky, G. Falkovich, I. Kolokolov, and V. Lebedev, Phys. Rev. Lett. **78**, 1452 (1997).
[7] W. E, K. Khanin, A. Mazel, and Ya. Sinai, Phys. Rev. Lett. **78**, 1904 (1997).
[8] W. E and E. Vanden Eijnden, Phys. Rev. Lett. **83**, 2572 (1999); Commun. Pure Appl. Math. **53**, 852 (2000).
[9] T. Gotoh and R. H. Kraichnan, Phys. Fluids **10**, 2859 (1998).
[10] T. Gotoh, Phys. Fluids **11**, 2143 (1999).
[11] R. H. Kraichnan, chao-dyn/9901023.
[12] J. Bec, Phys. Rev. Lett. **87**, 104501 (2001).
[13] U. Frisch and J. Bec, in *Les Houches 2000: New Trends in Turbulence*, edited by M. Lesieur, A. Yaglom, and F. David (Springer EDP-Sciences, New York, 2001), pp. 341–383.
[14] V. Gurarie, nlin.CD/0307033.
[15] V. Yakhot (private communication).
[16] R. J. LeVeque, *Numerical Methods for Conservation Laws* (Birkhäuser Verlag, Basel, 1992).
[17] C. F. von Weizsäcker, Astrophys. J. **114**, 165 (1951).
[18] C. M. Brunt, M. H. Heyer, E. Vázquez-Semadeni, and B. Pichardo, Astrophys. J. **595**, 824 (2003).